Magneto-optic and mechanical properties of TeO_2 with K_2TeO_3 doped with rare earth

K. I. Hussein[a,b,c], R. A. Al-Qahtani[d], N. Alzedanie[d], S. A. Muhammad[d], M. S. Alqahtani[a,b], I. S. Asiri[b*], M. Reben[f], E. Yousef[a,d]

[a]*Research Center for Advanced Materials Science (RCAMS), King Khalid University, Postcode: 9004, Zip code: 61413, Abha, Saudi Arabia*

[b]*Department of Radiological Sciences, College of Applied Medical Sciences, King Khalid University, Abha 61421, Saudi Arabia*

[c]*Department of Medical Physics and Instrumentation, National Cancer Institute, University of Gezira, Wad Medani 2667, Sudan*

[d]*Physics Department, Faculty of Science, King Khalid University, Postcode: 9004, Zip code: 61413, Abha, Saudi Arabia*

[e] *BioImaging Unit, Space Research Centre, Department of Physics and Astronomy, University of Leicester, Leicester LE1 7RH, UK*

[f]*Faculty of Materials Science and Ceramics, AGH – University of Science and Technology, al. Mickiewicza 30, 30-059 Cracow, Poland*

The novel glasses within composition: $62TeO_2$-$5K_2TeO_3$-$20ZnO$-$10Nb_2O_5$-$3PbF_2$ and $62TeO_2$-$5K_2TeO_3$-$20ZnO$-$10Nb_2O_5$-$3PbF_2$-$2Er_2O_3$ in mol% were fabricated by using melt-quenching technique. The magnetic properties *Viz;* Faraday effect and the Verdet constant at wavelength of laser beam (λ = 632 nm) were measured. The prepared sample with doped Er^{3+} has the highest value of Verdet constant (= 0.104min/G.cm) which depends on the polarizability of Er^{3+} ions. Moreover, the optical properties of present glass estimated by using UV-Vis-NIR spectroscopy. The oxygen-packed densities, molar volumes, the polarizability of the oxygen molar volume, the linear refractive index (n), third-order nonlinear susceptibility, $\chi^{(3)}$, and nonlinear index (n_2) of produced glasses were evaluation. It was found that the linear refractive index decreases otherwise the optical energy gap increased with doped Er^{3+} ions in the glasses network. Also, the Vickers microhardness increase with increasing Er_2O_3 in the glass matrix. Hence, these glasses may be use in optical isolator with high third-order non-linear susceptibility.

(Received November 16, 2022; Accepted February 3, 2023)

Keywords: Magnetic properties, Faraday effect, Structure tellurite, Refractive index, Polarizability, Microhardness

1. Introduction

For photonics applications, materials like rare earth-activated tellurite glasses are employed; optical amplifiers at 1.5 and 3.0 μm in telecommunication windows, and frequency up-converters [1, 2]. The composition of TeO_2-based glass systems is as follows; TeO_2-K_2O-Nb_2O_5, TeO_2-ZnO-Nb_2O_5, and TeO_2-Nb_2O_5-PbO have high value of nonlinear refractive indices, n_2, third-order susceptibility optical nonlinearity, $\chi^{(3)}$, resistance to crystallization, chemical durability as well as thermal stability [3, 4]. Tomokatsu et al. [5] found that, $\chi^{(3)}$, glasses decrease with increasing alkali oxide content moreover it increases with decreasing the optical band gap E_{opt}. A study of the, n_2, and β of Nb_2O_5–TeO_2 glasses, ZnO–Nb_2O_5–TeO_2 glasses, and MO–Nb_2O_5–TeO_2 (M = Mg, Ca, Sr, Ba) glasses. It was found that value of, n_2, and, β, increased (n_2= 2.0–2.9 $\times 10^{-14}$ cm^2/W, β=1.7-2.5 $\times 10^{-10}$ cm/W) by doping with alkaline-earth oxides MO (M = Mg, Ca, Sr, Ba) in

* Corresponding author: assiriebtesam22@gmail.com
https://doi.org/10.15251/JOR.2023.191.105

Nb_2O_5–TeO_2 glass (n_2= 1.49 ×10^{-14} cm^2/W, β=7.72 ×10^{-11} cm/W). The stretching band of Te–O_{ax} in TeO_4 (tbp) increased as the stretching band of Te–O in TeO_3 (tp) unit increased, whereas the stretching band of Te–O in TeO_3 (tp) unit and that of Te–O–Te declined, according to the connection between the glass structures. This means that the number of TeO_4 (tbp) units was directly proportional to the value of, $\chi^{(3)}$. Three different alkali metal oxides R_2O (R=Li, Na, K) as network modifiers and two network intermediates MO (M=Zn, Mg) are used to study third-order nonlinear optical characteristics in TeO_2-MO-R_2O glasses. These glasses have nonlinear refraction indices, n_2, are ranged from 1.31–2.81×10^{-15} cm^2/W. It was observed that when the ionic radius of both network modifiers and intermediates leads to the value of, n_2 increases.

The magneto-optical rotation of light's polarization is carried on by the Zeeman splitting of atomic energy levels [6]. A linearly polarized laser beam with left and right circularly polarized components will propagate at various rates in the desired direction through a magneto-optical material when a magnetic field is applied because they have different refractive indices. The incoming laser beam's plane of polarization spins as a consequence when a linearly polarized laser beam passes through such a material [7, 8]. The equation relates the rotational angle, θ, of glass to the magnetic field B, the Verdet constant (V), and the length of the glass, L, as follows [8].

$$\theta = VLB \tag{1}$$

where, $B = \frac{\mu_0 NI}{L_s}$, μ_0 is a constant of 1.26×10^{-6} Hm^{-1}, N is the turn numbers of a coil surrounding the solenoids, I. is the current go through the solenoids, L_s is the length of solenoids.

Therefore we investigated the density, Verdet constant, oxygen packing density, molar polarization, linear refractive index n, and Vicker's microhardness of prepared glasses to use in optical isolator devices.

2. Experimental work

The present glasses with composition: 62TeO_2-5K_2TeO_3-20ZnO-10Nb_2O_5-3PbF_2 (Sample A) and 62TeO_2-5K_2TeO_3-20ZnO-10Nb_2O_5-3PbF_2-2Er_2O_3 (Sample B) in mol% were prepared in a dry oxygen stream. The raw materials were melted in platinum crucibles at 990°C in a special temperature program with an air environment. At room temperature, samples were cast in a graphite mold, then annealed for 2 hours at 330°C. For spectroscopic investigations and optical measurements, the glasses sample was polished. For mechanical and optical measurements, the produced samples were polished as optical-flat.

The density of glass is being measured in order to better understand its physical features, which may then be connected to the composition change. The $g.cm^{-3}$ unit is used to measure it. The Archimedes technique was employed to estimate density since it requires more information about the properties of the glass and provides a more accurate result. The density of the liquid is known as ρ_L, while the weight of the glass sample is known as W_a in the air and W_L in the liquid. This relationship may be used to calculate the sample density, ρ_g:

$$\rho_g = \frac{W_a \cdot \rho_L}{W_a - W_L} \tag{2}$$

The hardness of a material is often linked with its resistance to abrasion or wear, and this property is useful since it may influence the material's durability and applicability for certain applications.

A substance's hardness is defined as its resistance to being penetrated by another rigid item [9]. Indentation is often assessed using glass and ceramics, according to Vickers. A sufficiently hard indenter is forced into the surface of the tested material, and the hardness, H, is calculated as the ratio of the load, F, to the total surface area, A of the permanent indentation, as shown in following equation.

$$H = \frac{F}{A} \quad (4)$$

The Vickers indenter [9] is a diamond pyramid with a 136^0 degree angle between opposing pyramid sides. The lengths l_1, l_2 of both diagonals of the indentation are measured after loading, stopping, and unloading the indenter. The Vickers hardness is determined by the relationship, H_v:

$$H_V = 0.1891 \cdot \frac{F}{l^2} \quad (3)$$

where, $l = \frac{l_1+l_2}{2}$ is the average of diagonal length (mm).

The wavelength range was 190-2500 nm, and the absorption spectra were obtained using a UV-VIS-NIR double beam spectrophotometer (JASCO V-570 spectrophotometer).

To investigate the amorphous nature of the quenched glass, we used X-Ray (CuKα) Powder Diffractometer Shimadzu model XRD-6000.

3. Results and discussion

3.1. XRD patterns of prepared glasses

X-ray diffraction patterns (XRD) of tellurite glasses with compositions of $62TeO_2$-$5K_2TeO_3$-$20ZnO$-$10Nb_2O_5$-$3PbF_2$ (Sample A) and $62TeO_2$-$5K_2TeO_3$-$20ZnO$-$10Nb_2O_5$-$3PbF_2$-$2Er_2O_3$ (Sample B). There are no strong peaks in these samples' patterns due to crystalline phases. The absence of strong diffraction peaks shows the absence of a crystalline phase, whereas the wide diffraction confirms the manufactured glasses' amorphous nature.

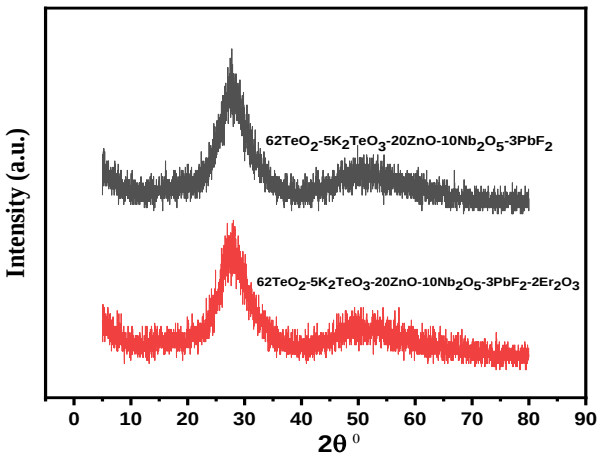

Fig. 1. XRD pattern of prepared glasses.

The length of samples with constant as a function of magnetic field B. The Verdet constant (V), which is determined by (slope = VL), is shown by the slope. For glass A and B, the values of the Verdet constant (at =632 nm) are 0.087 and 0.104 min./Oe.cm, respectively. The Verdet constant value are higher than those that have been previously reported in the literature [9, 10]. With paramagnetic erbium ions, the sample doped with erbium oxide (Er_2O_3) exhibits high V values, which led to the performance and increase in the angle of rotation of the light polarization plane under the influence of the magnetic field, which is consistent with the previously noted increase in magnetic susceptibility.

As a result, the paramagnetic response of Er in YAG is substantially greater than that in tellurite glass, most likely as a result of the host crystal's influence on the frequency of the paramagnetic dopant's electric dipole transition. The paramagnetic component of the Verdet constant is principally influenced by the concentration of the rare earth ion and the host glass in the instance of the magneto-optical influence of rare-earth ions in glasses.

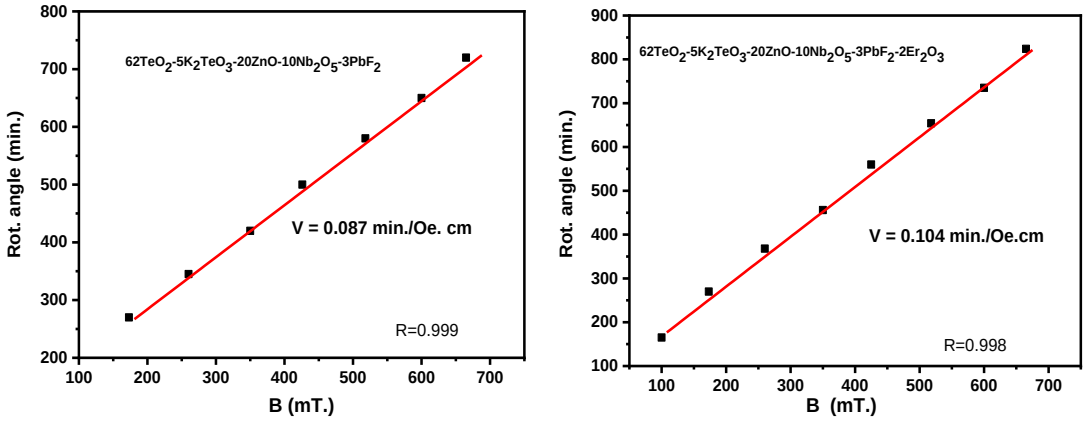

Fig. 2. (a) Relation between magnetic field B and Faraday rotation angle θ for the glass ($62TeO_2$-$5K_2TeO_3$-$20ZnO$-$10Nb_2O_5$-$3PbF_2$) in mol%; (b) Relation between magnetic field B and Faraday rotation angle θ for the glass ($62TeO_2$-$5K_2TeO_3$-$20ZnO$-$10Nb_2O_5$-$3PbF_2$-2 Er_2O_3) in mol%.

3.2. Optical properties and Vickers microhardness of prepared glasses

The values of molar volume, V_m, $V_m = \frac{\sum_i x_i m_i}{\rho}$, molar volume of oxygen, V_O, $V_o = (V_m).\left(\frac{1}{x_i\, n_i}\right)$, and oxygen packing density, $O.\ p.\ d$, $O.p.d = \sum_i \frac{1000\ .\ \rho\ .\ n_i}{m_i}$,

where x_i denotes the molar percentage of each oxide component, m_i denotes the glassy composition's molecular weight, and n_i denotes the number of oxygen atoms in each oxide. These factors are used to investigate whether the network of current glasses is dense or weak, and the findings are described in Table (2). When the concentration of Er^{3+} ions is increased from 0 to 20000ppm, the density increases from 5.5713 to 5.5816 gm cm^{-3}. V_m and V_o, on the other hand, are directly connected to the spatial distributions of oxygen in the glass matrix, increasing from 29.051 to 30.369 cm3 and from 13.9 to 14.125 cm^3mol^{-1}, respectively. When Er^{3+} is increased from 0 to 20000ppm, the O.p.d. value reduces from 71.942 to 70.797 $gmatmL^{-1}$. The density value is impacted by the molecular weight of the constituent for glasses composition, the coordination numbers with interstitial spaces, and the crosslink density of the glass composition, and it is connected to changes in the structure of produced glasses. The addition of the heavy ions Er3+ causes the network of glasses to expand, resulting in an increase in density. When Er^{3+} ions are added to the host glass (Sample A), the rate of change in molecular weight is larger than the rate of change in density value. The greater values of the ionic radii and creation free ions of Er^{3+} solubility in the host glass matrix may be ascribed to the rise in Vo and reduction in O.p.d of the produced glasses.

Table 1. Density, ρ, molar volume Vm, oxygen molar volume, V, optical packing density, o.p.d, energy gap E_{opt}, and refractive index, (n) of prepared glasses.

Sample code	Density, ρ (g/cm^{-3})	Molar volume V_m (cm^3)	Oxygen molar volume, V_o (cm^3)	O.p.d g.atom.l^{-1}
Sample A	5.5713	29.051	13.9	71.942
Sample B	5.5816	30.369	14.125	70.797

Figures (2a) and (2b) show the UV–Vis–NIR absorption spectra of the prepared glasses (3. 2B). According to the influence of codoped Er3+ ions in the host glasses $62TeO_2$-$5K_2TeO_3$-$20ZnO$-$10Nb_2O_5$-$3PbF_2$, absorption bands in the UV-VIS-NIR regions develop, and we may easily be assigned. The energy levels of the transition in the glass matrix correspond to the absorption.

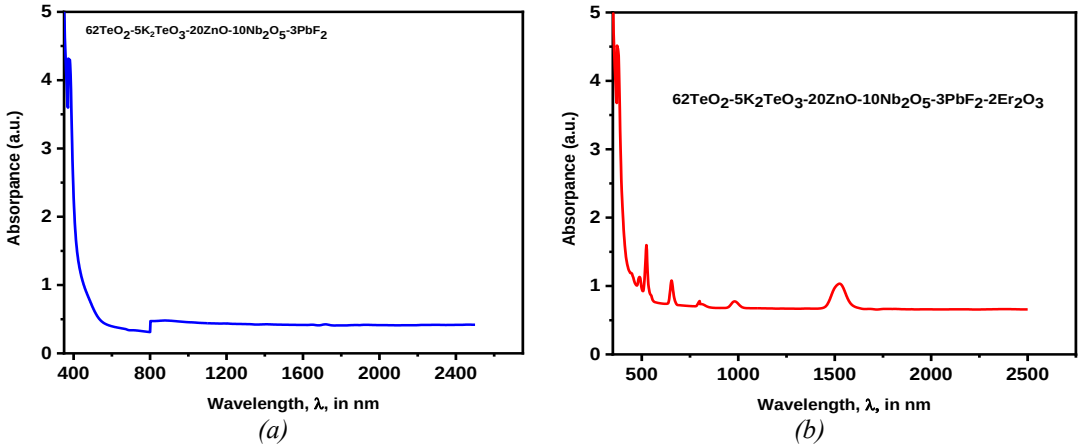

Fig. 3. (a) Absorbance spectra of the glass ($62TeO_2$-$5K_2TeO_3$-$20ZnO$-$10Nb_2O_5$-$3PbF_2$) in mol%; (b) Absorbance spectra of the glass ($62TeO_2$-$5K_2TeO_3$-$20ZnO$-$10Nb_2O_5$-$3PbF_2$-2 Er_2O_3) in mol%.

The optical absorption coefficient α(ν) $\alpha(\nu) = \frac{1}{d}\ln\left(\frac{I_o}{I_t}\right) = \frac{2.303\,.\,A}{d}$, where, ν,, where is the light beam frequency, I_0 and I_t are the incident and transmitted beam intensities, A, is the optical absorbance, and, d, is the glass sample thickness in cm. Furthermore, is associated to, as, where E_{opt} is the optical band gap energy in eV, B is a constant, and the exponent, r, is an index whose values of 1/2 and 2 greatly dependent on the mechanism type of electronic transition that causes absorption. Where r is equal to 1/2 for direct transitions permitted and 2 for indirect transitions allowed. Because the indirect transitions happened according to the Tauc relations [13], we assumed r= 2 in glassy materials. Extrapolation of the linear area of the against photon energy graphs at =0 (see Fig. (4a) yielded the values of indirect optical band gap energy E_{opt} (see Fig.4b).

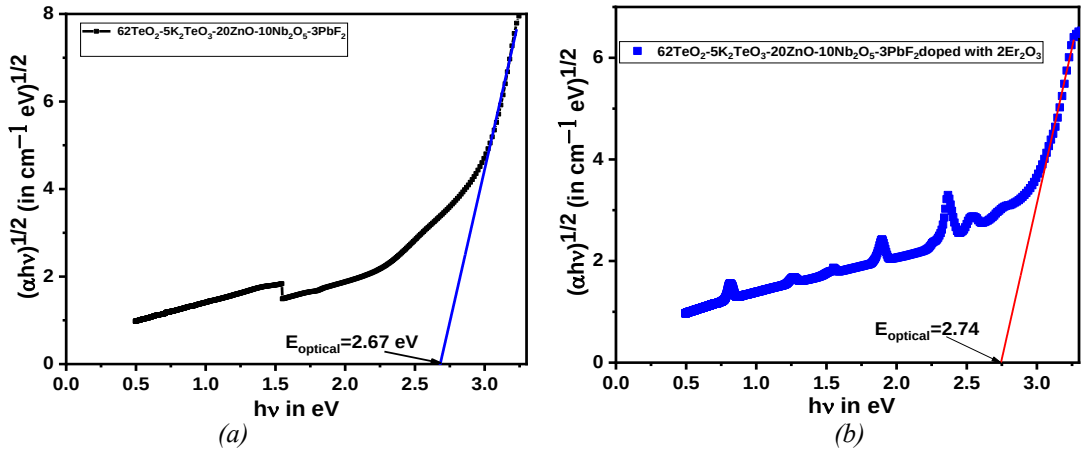

Fig. 4. (a) $(\alpha h\nu)^{1/2}$ versus $h\nu$ of of the glass ($62TeO_2$-$5K_2TeO_3$-$20ZnO$-$10Nb_2O_5$-$3PbF_2$) in mol%; (b) $(\alpha h\nu)^{1/2}$ versus $h\nu$ of of the glass ($62TeO_2$-$5K_2TeO_3$-$20ZnO$-$10Nb_2O_5$-$3PbF_2$-$2Er_2O_3$) in mol%

Depending on the amount of Er^{3+} ions doped in the host glasses sample A, the E_{opt} value increases from 2.67 to 2.74 eV. (See column 2 in Table 2).

Optical factors such as linear refractive indices, n, non-linear refractive indices, n_2, and third-order susceptibility are significant in the manufacturing of optical devices, $\chi^{(3)}$. With increasing doped Er^{3+} ions from 0 to 20000ppm, the linear refractive index decreased from 2.492 to 2.471. Which, n, is greatly influenced by the ion density and polarizability in the glass network.

The molar refraction, R_m, $R_m = V_m \cdot \frac{n^2-1}{n^2+2}$, and molar polarizability, α_m, $\alpha_m = \frac{3}{4\pi N_A V_m} \cdot \left(\frac{n^2-1}{n^2+2}\right)^{-1}$ [1- 3], Avogadro's number is N_A. With increasing doped Er_2O_3 from 0 to 20000ppm in the host glass (sample A), the, R_m, and α_m values increase from 18.437 to 19.128 in cm^3mol^{-1} and from 7.319 to 7.591 in A^{03}, respectively (See column 3 in Table 2).

The value of metallization criterion, M_c, of fabricated glasses as follow; $M_c = 1 - \frac{n^2-1}{n^2+2}$. With increasing doped Er_2O_3 from 0 to 20000ppm in the prepared glasses, the value M_c increases from 0.365 to 0.37.

Table 2. Energy gap E_{opt}, and refractive index, (n) of prepared glasses.

Sample code	Energy gap, E_{opt}, in eV	Refractive index, (n)	Molar polarizability, α_m, ($Å^3$)	Molar refraction, R_m, (cm^3/mol)	Metallization criterion, M_e
Sample A	2.67	2.492	7.316	18.437	0.365
Sample B	2.74	2.471	7.591	19.128	0.37

The linear optical susceptibility may be used to calculate the third-order nonlinear optical susceptibility, $\chi^{(3)}$. As follow;

$\chi^{(3)} = 1.7\left[\chi^{(1)}\right]^4 \times 10^{-10}\ esu$, where $\chi^{(1)} = \frac{(n^2-1)}{12.56}$. The, $\chi^{(3)}$, values of prepared glasses are reported in table (3- 3), its decrease from from 5.036 to 4.64 x 10^{-13} esu. The value of nonlinear refractive index, n_2, was evaluated as follow; $n_2 = \frac{12\pi\chi^{(3)}}{n}$; it decreases from 7.61 to 7.07×10^{-11} esu with increasing Er_2O_3.

The created glass was tested for Vickers hardness. Table 3 summarizes the findings results. The Vickers hardness, H_v, increases as the proportion of Er_2O_3 in the composition increases, as seen in the table. It's due to the glass network being more tightly packed, which makes the glass matrix stronger [11].

Table 3. The real third-order non-linear susceptibility $\chi^{(3)}$, of prepared glasses.

Sample code	$\chi^{(3)} \times 10^{-12}$ (esu)	nonlinear refractive indices,n_2, $\times10^{-11}$in esu	Vicker,s Microhardness, Hv, in GPa
Sample A	5.036	7.61	5.3
Sample B	4.64	7.07	5.32

4. Conclusion

In this work, we report optical and mechanical properties of prepared glasses with composition: $62TeO_2$-$5K_2TeO_3$-$20ZnO$-$10Nb_2O_5$-$3PbF_2$ and $62TeO_2$-$5K_2TeO_3$-$20ZnO$-$10Nb_2O_5$-$3PbF_2$-$2Er_2O_3$ in mol%. The E_{opt} value increase from 2.67 to 2.74 eV depending on the Er^{3+} ions concentration doped the host glasses sample A. With increasing doped Er^{3+} ions from 0.0 to 20000ppm, the linear refractive index decreases from 2.492 to 2.471. The, R_m, and α_m values increase from 18.437 to 19.128 in $cm^3 \cdot mol^{-1}$ from 7.316 to 7.591 in A^{03} with increasing doped Er_2O_3 from 0.0 to 20000ppm in the host. The Verdet constant increase of glass doped with Er^{3+} from 0.087 to 0.104 min./Oe.cm. Otherwise, the third-order nonlinear optical susceptibility, $\chi^{(3)}$, decreases from 5.036 to 4.64 x 10^{-12} esu of prepared glasses. The Vickers microhardness increased from 5.3 to 5.32 GPa with incorporated Er^{3+} ions in the glass matrix.

Acknowledgments

This work was supported by the King Khalid University through a grant RCAMS/KKU/04-22 under the Research Center for Advance Materials (RCAMS) at King Khalid University, Saudi Arabia

References

[1] El S. Yousef, M. M. Elokr, Y. M. Aboudeif, Chalcogenide Letters 12, 597 (2015).

[2] A. M. Emara, M. M. Alqahtani, Y. M. Abou Deif , El Sayed Yousef, Chalcogenide Letters 14, No. 9, 405, (2017).

[3] Y. M. Aboudeif, M. M. Alqahtani, A. M. Emara, H. Algarni, El S. Yousef, Chalcogenide Letters 15, 219 (2018).

[4] E. Golis, El S. Yousef, M. Reben, K. Kotynia, and J. Filipecki. Solid State Sciences 50 (2015): 81-84; https://doi.org/10.1016/j.solidstatesciences.2015.10.017

[5] M.I Sayyed, F. Laariedh, , A. Kumr, et al. Experimental studies on the gamma photons-shielding competence of TeO2-PbO-BaO-Na2O-B2O3 glasses. Appl. Phys. A 126, 4 (2020); https://doi.org/10.1007/s00339-019-3182-8

[6] M. Kamislioglu, E.E. Altunsoy Guclu, & H.O. Tekin, Comparative evaluation of nuclear radiation shielding properties of xTeO2 + (100-x) Li2O glass system. Appl. Phys. A 126, 95 (2020); https://doi.org/10.1007/s00339-020-3284-3

[7] E. Yousef, M. Hotzel, C. Rüssel. Linear and non-linear refractive indices of tellurite glasses in the system TeO2-WO3-ZnF2,Journal of Non-Crystalline Solids, Volume 342, Issues1-3,2004, 82-88; https://doi.org/10.1016/j.jnoncrysol.2004.07.003

[8] A. M. Alqahtani, M. S. Alqahtanib, K. I. Hussein, A. J. Alkulib,F. F. Alqahtani, N. Elkhoshkhany, I. S. Yaha, M. Reben, E. Yousef. Study of ionizing radiation attenuation of glass as: gamma rays shielding material, Chalcogenide Letters, Chalcogenide Letters Vol. 19, No. 4, April 2022, p. 227 - 239.

[9] A. Z. Alzuhaira , M. S. Alqahtania, A. J. Alkuliba, K. I. Hussein, M. Reben, E. Yousef. Structural and shielding properties of the tellurite-tungsten glass matrix with addition zinc fluoride Chalcogenide Letters Vol. 19, No. 3, 2022, 187- 195; https://doi.org/10.15251/CL.2022.193.187

[10] A. M. Alqahtani , M. S. Alqahtani, K. I. Hussein, A. J. Alkulib , F.F. Alqahtani, E.Yousef, Radiation protection assessment of gamma photons in 64TeO2-10WO3-10Nb2O5- 15KF-1La2O3 glasses doped with Tm2O3 using photon-shielding and dosimetry software Chalcogenide Letters Vol. 18, No. 9, September 2021, p. 513 - 523.

[11] T. Hayakawa, M. Hayakawa, M. Nogami, P. Thomas, Optical Materials, 32 (3), 448, (2010); https://doi.org/10.1016/j.optmat.2009.10.006

[12] T.J. Kane, R.L. Byer, Opt. Lett. 10, 65 (1985); https://doi.org/10.1364/OL.10.000065

[13] B. Yao, X. Duan, D. Fang, Y. Zhang, L. Ke, Y. Ju, Y. Wang, G. Zhao, Opt. Lett. (2008) 33, 2161; https://doi.org/10.1364/OL.33.002161

[14] A. M. Al-Syadi, M. Alfarh, H. Algarni, M. S. Alqahtani, M. Reben, H. Afifi, El Sayed Yousef, Chalcogenide Letters, Vol. 18, No. 9, September 2021, p. 541 - 54

[15] Lachlan Harris, David Ottaway, Peter J. Veitch, Appl Phys B (2012) 106:429-433; https://doi.org/10.1007/s00340-011-4761-3

[16] A. Grishin, V. A. Gur'ev, E. B. Intyushin, Yu. E. Elliev, O. V. Pavlova, and A. P. Savikin, Russian Journal of Applied Chemistry, Vol. 77, No. 8, 2004, pp. 1245; https://doi.org/10.1007/s11167-005-0007-7

[17] M. Joshia, A. Bhattacharyya, S. Ali, Indian journal of fiber &Textile Research 33, 304, (2008).

[18] Mencik, J. Strength and Fracture of Glass and Ceramics. Glass Science and Technology.1992. Volume (12): 156-157.

[19] Tauc, F. Urbach, Physical Review A 92 ,1329(1953); https://doi.org/10.1103/PhysRev.92.1324